Research Article

Fei Li*, AnZhong Deng, QiLin Zhao, and Jinhui Duan

Research on Influence mechanism of composite interlaminar shear strength under normal stress

https://doi.org/10.1515/secm-2020-0011
Received Nov 18, 2019; accepted Mar 05, 2020

Abstract: The normal stress along the shear plane has great effect on the composite intralaminar shear strength. However, the influence mechanism on composite interlaminar shear strength under the normal stress along the shear plane was not truly reflected by the double-notch shear experiment. In this paper, the interlaminar shear strength of composite specimens under different external normal stresses was first obtained using the improved double-notch shear experiment. Furthermore, to research the influence mechanism on interlaminar shear strength under normal stress along the shear plane, the characteristic curve method based on the double-notch shear specimen was studied. Finally, the experimental results analyzed by the characteristic curve method were compared with a range of failure criteria presented in the literature. The experimental data obtained in this study agreed best with the NU theory criterion, with a maximum numerical difference of 4%. And the NU theory criterion can reflect the influence mechanism of the composite interlaminar shear strength best.

Keywords: Composite connection; Normal stress; Interlaminar shear strength; Characteristic curve method; Influence mechanism

1 Introduction

With the increasing use of composite for large load-bearing structures, the stress state of materials has become more complicated [1–4]. Through-thickness compressive loadings can arise from normal stress as found in composite joints. The normal stress has a significant influence on bearing capacity of composite joint, *i.e.* the compressive normal stress can increase the bearing capacity of composite bolt joint [5–8]. During force transmission, the composite pre-tightened tooth connection is subjected to the effect of both interlaminar shear stress and normal stress. Under the effect of compressive normal stress, the joints can transmit a larger load [9]. However, the tensile normal stress can weaken the bearing capacity of composite joint. Most shear damages of composite adhesive joint are caused by the tensile normal stress along the shear plane and shear stress.

Currently, the influence on interlaminar shear strength under normal stress is mainly focused on experimental research. McManamy *et al.* showed an increase in interlaminar shear strength with compression for small specimens of 2D woven S-glass in bismaleimide resin using a biaxial experiment [10]. DeTeresa *et al.* studied the effect of through-thickness compression on interlaminar response for five different glass and carbon fibre-reinforced composites using hollow cylindrical specimens loaded with combined torsion and a predetermined compressive force [11]. Hine *et al.* showed an increase in interlaminar shear strength for unidirectional (UD) glass/epoxy under hydrostatic pressures using 10 off-axis tensile experiments [12]. Koerber *et al.* used a similar approach. however, they varied the fibre angle instead of the fixture and performed off-axis end-loading compression experiments on Hexcel IM7/8552 carbon/epoxy prepreg with fibre orientation angles θ=15°, 30°, 45°, 60°, 75°, and 90°. An increase of 40% was observed in the in-plane shear strength for combined transverse compression and in-plane shear loading [13]. Some limitations of the experimental tests mentioned above. The shear stress and normal stress in this type of experiment specimens were mainly adjusted by changing the fibre orientation angle and the fixture angle, which determined the ratio of shear to compressive load on the specimens. When a large amount of experimental data is required, this type of experiment requires constant changes in the fibre or fixture angle of the exper-

***Corresponding Author: Fei Li:** College of Civil Engineering, Chongqing Jiaotong University, Chongqing 400074, China; Email: lifei609@163.com
AnZhong Deng: Army Logistics University of PLA, Chongqing 400001, China
QiLin Zhao: School of Mechanical and Power Engineering, Nanjing University of Technology, Nanjing 21007, China
Jinhui Duan: Engineering Institute of Engineer Corps, PLA University of Science and Technology, Nanjing 210007, China

iment specimen. To overcome these shortcomings, Khong *et al.* performed direct measurement of interlaminar shear strength under moderate external normal stress by the double-notch shear experiment, which further proved the enhancement effect of compressive normal stress on interlaminar shear strength [14]. By the double-notch shear experiment, normal stress can be directly changed on the same type of experiment specimen, which effectively overcomes the shortcomings of experiment mentioned above. In the double-notch shear experiment, there are external normal stress applied by the experiment equipment and normal stress along the shear plane which is shown in Figure 1. The damage of the final experiment specimen is the result of the combined effect of normal stress and shear stress along the shear plane. However, in a study by Khong *et al.*, a direct relationship between external normal stressand interlaminar shear strength was obtained. The normal stress along the shear plane was neglected. Thus, influence mechanism on composite interlaminar shear strength under the normal stress was not truly reflected.

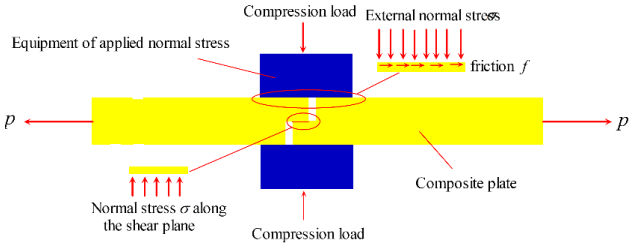

Figure 1: Double-notch shear specimen

To further research the influence mechanism on composite interlaminar shear strength under the normal stress, the existing double-notch shear experiments were first improved and the external normal stress application device is simplified, which considerably reduced the requirements for the experiment machine. Furthermore, to study the influence of normal stress along the shear plane on interlaminar shear strength, the characteristic curve method based on the double-notch shear specimen is proposed. Finally, the obtained experimental results were compared with the failure criteria.

2 Materials and Methods

2.1 Experimental improvement

Testing interlaminar shear strength using an existing standard double-notch shear experiment specimen has the following shortcomings. The double-notch shear specimen is generally loaded by clamping its two ends with the experiment machine. If the clamping force at both ends is too large, the experiment specimen may get crushed. However, if the clamping force at both ends is too small, there might be a slip between the chuck and the experiment specimen. In addition, clamping the specimen using chucks could easily generate a bending moment when applying force to the experiment specimen. The experiment specimen may break in advance under the effect of the bending moment, resulting in a relatively small measured interlaminar shear strength. In this study, the double-notch shear experiment was redesigned to address the above-mentioned problems. As shown in Figure 2, holes were made at both ends of the composite experiment specimen, and then the composite experiment specimen and the external metal conversion joint were assembled by bolts. The connection between the experiment specimen and the experiment machine was realised by the metal conversion joint. While preparing the experiment specimen, the centre of the composite experiment specimen hole and the shear plane should be kept on the same plane as much as possible. The hole diameter on the experiment specimen was slightly larger than the bolt diameter to ensure that the experiment specimen could rotate freely under the external load. This would not only overcome the problem of clamping the end of the experiment specimen, but also eliminate the influence of the bending moment on the experiment specimen. The application device for the external normal stress of the experiment specimen is shown in Figure 3. As shown, steel plates with screw holes are arranged on both sides of the shear zone of the composite experiment specimen. The steel plates and the composite material experiment specimen are fixed by bolts. A torque was applied to the bolt to make the external steel plates press on the composite experiment specimen, thereby achieving the application of external normal stress. The magnitude of normal stress on the experiment specimen can be adjusted by applying a torque to the bolt. To minimise the influence of deforma-

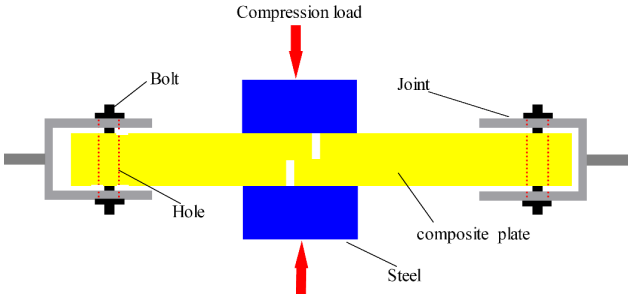

Figure 2: Conversion joint design

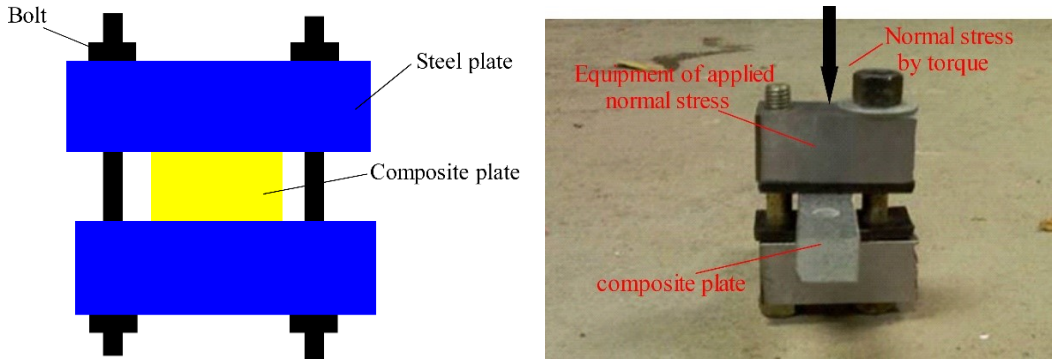

Figure 3: The external normal stress application device design

Table 1: Material properties of composite

E_1	E_2	E_3	ν_{12}	ν_{23}	ν_{13}	G_{12}	G_{23}	G_{13}	S_2^+	S_2^-	S_{12}
30GPa	14GPa	14GPa	0.0485	0.0485	0.0485	7.4GPa	5.5GPa	7.4GPa	30GPa	160GPa	32GPa

Note, 1 is the along fiber direction, whereas 2 and 3 are perpendicular to the fiber directions. S_2^+ and S_3^- are the tensile and compressive strength along the fiber direction, S_{12} is the shear strength along the fiber direction.

tion of the steel plate, and to make the application of external normal stress force uniform, it is necessary to increase the rigidity of the steel plate by increasing its thickness. The biggest advantage of this method as compared to that proposed by Khong *et al.* is that it is simple to apply external normal stress, and the experiment can be performed on a common material testing machine [14].

2.2 Specimen

The carbon fibre composite material used in this study was pultruded for the experiment. Vinyl ester resin was selected as the matrix. The fibre fractions were approximately 50% per weight, of which approximately 89.15% was carbon fibre and 10.85% was combined mats. The material parameters are presented in Table 1.

The notch spacing in a double-notch shear experiment have a large impact on the experiment results. The difference between the average shear strength and the maximum shear stress value increases with the increase of the notch spacing. Using smaller notch spacing will obtain a result closer to the true value. Therefore, choosing reasonable notch spacing has a large impact on the results of the experiment. In this experiment, the experiment specimen has a width of 22 mm, thickness of 17 mm, and length of 100 mm. According to the finite element study, when the shear length was 4 mm, the shear stress distribution on the shear surface was most uniform. Therefore, the shear surface length of the experiment specimen was determined to be 4 mm. Considering the feasibility of the processing, the notch width was also determined to be 4 mm, as shown in Figure 4. And Figure 5 shows the processed experiment specimen.

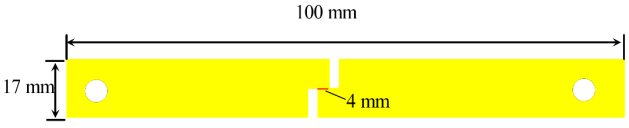

Figure 4: Geometric size of the experiment specimen

Figure 5: Experiment specimen

The tensile failure loads of specimens were measured at different torque values of 0, 5, 9, 13, 17, 21, and 25N·m (corresponding to the external normal stress values of 0, 6.3, 11.3, 16.4, 21.5, 27.5, and 32.3MPa on the steel plate, respectively). The experiment was performed on an electronic universal testing machine, as shown in Figure 6. The testing machine was controlled by a computer. The data was collected automatically and saved as a data file. The loading speed was 0.004 mm/s according to the ASTMD3846-94 standard. Each group of experiment specimens was numbered according to different the external normal stresses. The experiment results are presented in Table 2. It can be seen that as the external normal stresses

Table 2: The result of experiment

Serial number	External normal stress (MPa)	Failure load (kN)	Mean failure load (kN)	Failure model
T-0-1		2605.88		Shear failure
T-0-2		2366.63		Shear failure
T-0-3	0	2775.199	2506.822	Shear failure
T-0-4		1789.657		Shear failure
T-0-5		2996.744		Shear failure
T-6.3-1		3101.694		Shear failure
T-6.3-2		3312.532		Shear failure
T-6.3-3	6.3	3267.321	3201.694	Shear failure
T-6.3-4		3393.452		Shear failure
T-6.3-5		2933.471		Shear failure
T-11.3-1		3402.214		Shear failure
T-11.3-2		3923.542		Shear failure
T-11.3-3	11.3	4012.763	3802.214	Shear failure
T-11.3-4		3809.345		Shear failure
T-11.3-5		3863.206		Shear failure
T-16.4-1		3859.888		Shear failure
T-16.4-2		4427.554		Shear failure
T-16.4-3	16.4	4359.142	4259.888	Shear failure
T-16.4-4		4498.023		Shear failure
T-16.4-5		4154.833		Shear failure
T-21.5-1		4973.68		Shear failure
T-21.5-2		4894.235		Shear failure
T-21.5-3	21.5	5106.342	4973.68	Shear failure
T-21.5-4		5204.567		Shear failure
T-21.5-5		4689.576		Shear failure
T-27.5-1		5734.502		Shear failure
T-27.5-2	27.5	5635.254	5621.405	Shear failure
T-27.5-3		5494.459		Shear failure
T-32.3-1		6324.637		Shear failure
T-32.3-2	32.3	6197.201	6207.688	Shear failure
T-32.3-3		6101.226		Shear failure

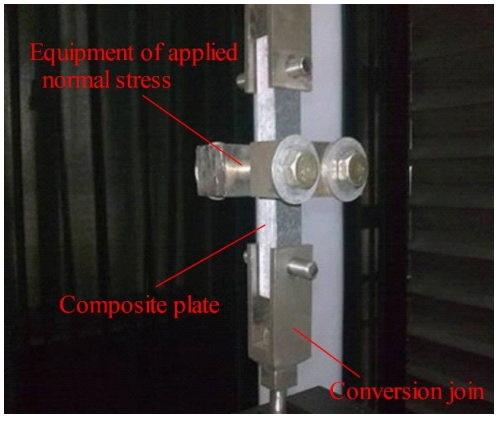

Figure 6: Specimen loading

increased, the ultimate load of the experiment specimen continued to increase.

Figure 7 shows the load-displacement curve of a tensile experiment specimen without applying external normal stress. It can be seen from the figure that during the initial loading, the surface structure did not appear to change, and abnormal sounds were not heard. As the load increased, subtle but continuous noise, which indicated damage, could be heard. Subtle horizontal cracks appeared at the front of the specimen notch and then quickly developed towards the back. After the crack developed to the entire shear plane, the specimen was damaged, which was accompanied by a loud sound. The final failure mode of the specimen is shear failure. Figure 8 shows the load-displacement curve of a tensile experiment spec-

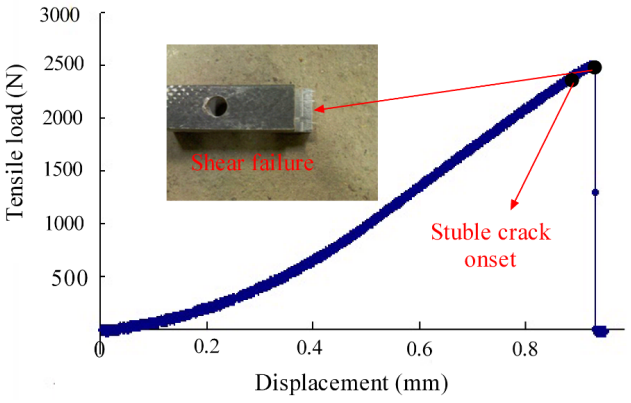

Figure 7: Load-displacement curve without external normal stress

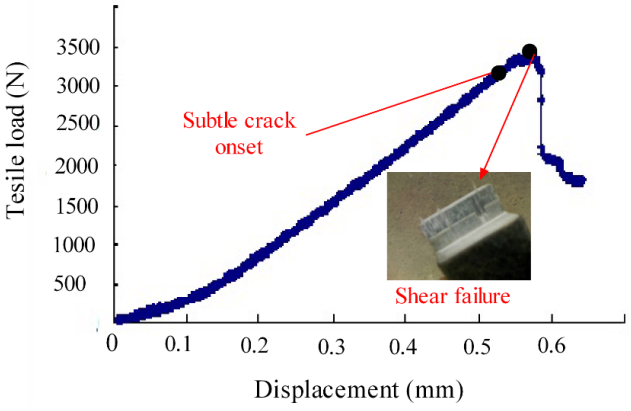

Figure 8: Load-displacement curve with an external normal stress of 11.3 MPa

imen when applying an external normal stress of 11.3MPa. It can be seen from the figure that during the initial load, the relationship between the load and displacement increased monotonically. The specimen did not appear to change, and abnormal sounds were not heard. As the load increased to3400N, subtle but continuous noise, which indicated damage, could be heard. Eventually, subtle cracks appeared. When the load increased to 3600N, shear failure occurred in the experiment specimen. After the specimen failure, the friction between the external normal stress application device and the composite experiment specimen caused the load of the specimen to be stable after the load was reduced to a certain extent. It can be observed from the load-displacement curve of the specimen that after applying external normal stress, the specimen transmitted the load both through the shear stress on the shear plane and through the frictional force. Therefore, while analysing the influence of normal stress on interlaminar shear strength, the effect of friction should be eliminated.

The interlaminar shear strength τ is simply calculated as the maximum shear load carried by the specimen during the test:

$$\tau = \frac{P_{\max}}{bl} \tag{1}$$

Where b is the width of the experiment specimen, and l is the length of the specimen shear plane.

Table 3: Interlaminar shear stresses under different external normal stresses

Serial number	External normal stress (MPa)	Shear strength (MPa)
T-0	0	28.49
T-6.3	6.3	36.38
T-11.3	11.3	43.21
T-16.4	16.4	48.41
T-21.5	21.5	56.52
T-27.5	27.5	63.88
T-32.3	32.3	70.54

The Table 3 shows the interlaminar shear strength of the specimen under different corresponding external normal stresses(without eliminating the effects of friction). It can be observed from Table 3 that as the external normal stress increased, the shear strength increased significantly. When the external normal stress was 0MPa, the shear strength was 28.49MPa. When external normal stress was 32.3MPa, the shear strength was 70.54MPa, which is three times the shear strength without external normal stress. This conclusion is consistent with that provided by Khong*et al.* [14], which demonstrated the validity of this experimental method. However, the results did not consider the influence of normal stress on the shear plane and the interfacial friction force. Therefore, the relationship established by external normal stress and the shear strength was not reasonable, and the experiment data must be analysed further.

3 Results and Discussion

3.1 Characteristic length determination

For the strength analysis of the composite hole with stress concentration, the most widely-used method in engineering is the characteristic curve method. The characteristic curve method was proposed by Whitney and Nuismer. Chang *et al.* developed their method on this basis [15]. A study by Li *et al.* showed that the bearing capacity of composite pre-tightened tooth connection could be effectively predicted by the characteristic curve method [16]. Based on the characteristic curve of the composite pre-

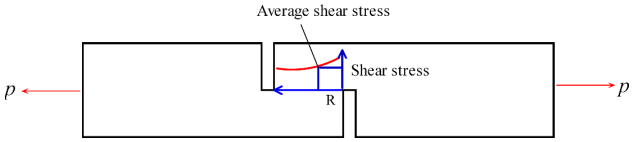

Figure 9: Schematic diagram of the characteristic length determination method

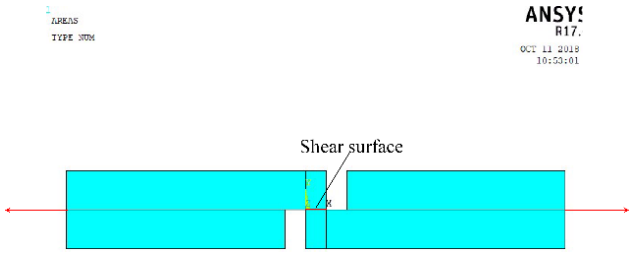

Figure 10: Finite element model of a double-notch shear specimen

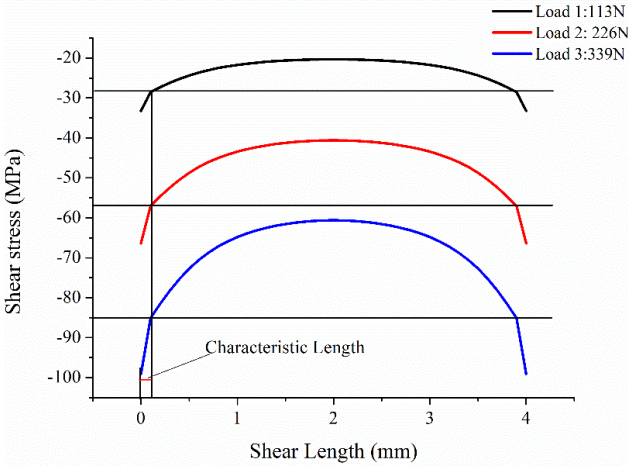

Figure 11: Characteristic length determination method

tightened tooth connection, Figure 9 shows the concept of the method to determine the characteristic length of the double-notch shear specimen. A typical pattern of the shear stress distribution along the shear surface under an arbitrary load P is obtained by the finite element model. The average shear stress τ by an arbitrary load P is calculated by Eqn 1.

The shear characteristic length of a double-notch shear specimen is defined as the distance from notch end with maximum shear stress to a point at which the shear stress is equal to the average shear stress under any tensile load.

An example to demonstrate the concept of the characteristic length determination method is shown in Figure 10. The laminate is modelled by the PLANE82 element in ANSYS. To demonstrate the present numerical method, an arbitrary load P is applied. The load is transferred by the shear stress of the shear surface. The material parameters are presented in Table 1. Figure 11 shows the characteristic lengths R when a load P of 113, 226, and 339 N is applied. When an arbitrary load P of 113 N is applied, the average shear stress along the shear surface is 28 MPa. Using the definition, the corresponding characteristic length R is calculated to be 0.4 mm under the load of 28 MPa. Similarly, the corresponding characteristic lengths can be obtained when a load P of 226 and 339 N is applied. The results in this example show that regardless of the applied load, the corresponding characteristic length does not change. Therefore, the characteristic length can be determined using an arbitrary load P.

3.2 Finite element analysis

To obtain stress distribution on the shear plane of the specimen, in this section, the specimen is modelled by ANSYS. The stress distribution of the composite shear plane under different external normal stresses is obtained. Considering that the composite material used in the experiment was made by pultrusion and there was no influence of layering, the composite laminate and the metal plate are modelled by the plane 42 element in ANSYS. Non-linear contact analysis is performed for the experiment specimen to consider the change of the contact surface during deformation. The friction coefficient is 0.3 in this model, and the element-size of the model is 0.2mm [17]. The geometry of the model was the same as the geometry of the experiment specimen being experimented in this study. The elastic modulus of steel was 2.1e5MPa in the model. The material parameters of the composite are presented in Table 1. Boundary conditions for the simulations were identical to the test conditions. a tensile force was exerted on the ends of composite, and a pretightening force was exerted between the top and bottom steel plates. Figure 12 shows the established finite element model.

Figures 13 and 14 show the normal stress distribution and the shear stress distribution on the shear plane of the double-notch shear specimen, respectively, under different external normal stresses and ultimate load calculated by ANSYS. It can be seen from the figures that the shear stress distribution on the specimen shear plane was relatively uniform under different external normal stresses, while the normal stress distribution on the shear plane was not uniform. However, both the normal stress and shear stress distribution trends were large in the ends and small

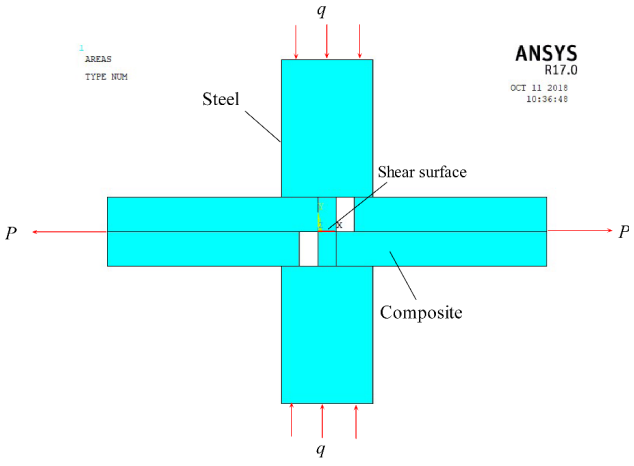

Figure 12: Finite element model

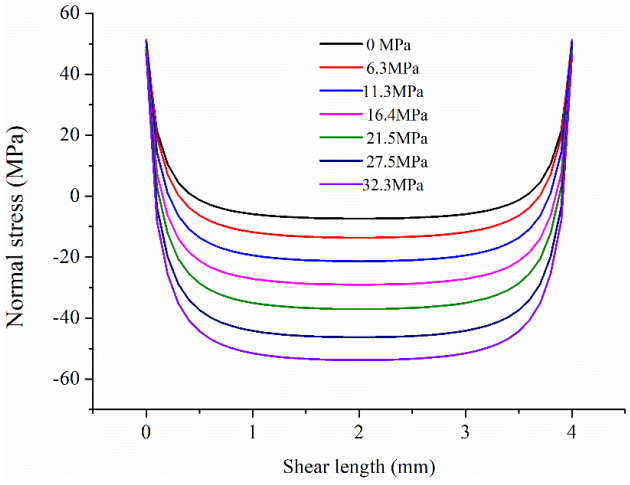

Figure 13: Normal stress distribution of specimen under different external normal stresses

in the centre, *i.e.* there was a stress concentration phenomenon at both the ends of the specimen.

The stress states of the characteristic points of the experiment specimen under different external normal stresses and ultimate loads were extracted. The results presented in Table 4 show that normal stress had a large impact on shear strength on the shear plane. When the tensile normal stress was 6.49 MPa, the corresponding shear strength was 29.73 MPa. When the compressive stress was 26 MPa, the shear strength was 49 MPa. In these two different normal stress states, the shear strength was increased by 60%. This means that as normal stress on the shear plane converted from tensile stress to normal stress, the shear strength of the experiment specimen enhanced continuously.

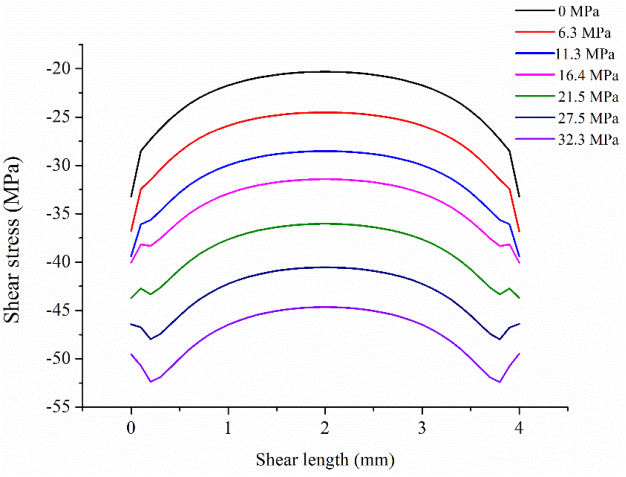

Figure 14: Shear stress distribution of specimen under different external normal stresses

Table 4: Shear stresses and normal stresses at the characteristic points

External normal stress (MPa)	Normal stress at the characteristic points (MPa)	Shear stress at the characteristic points (MPa)
0	6.4868	29.73
−6.3	4.9965	32.6812
−11.3	−0.8575	35.4505
−16.4	−5.928	37.4642
−21.5	−13.5426	41.0625
−27.5	−20.6275	44.6023
−32.3	−26.3866	49.4291

Note: the stress is under the tensile condition, when the stress value is positive. The stress is under the compression condition, when the stress value is negative.

3.3 Failure criteria

Through years of research, different failure criteria for the influence mechanism of normal stress on interlaminar shear strength have been proposed. In this study, some experimentally-validated criteria will be introduced, and the resultant experimental data will be compared.

Puck and Schürmann introduced a phenomenological failure criterion for interfibre fracture at unidirectional ply level under biaxial in-plane loading [18]. In particular for mode B fracture, in which the normal compressive σ_{33} impedes fracture because of shear σ_{31} i on the fracture plane where the fracture angle $\theta_{fp} = 0°$ the fracture condition in the 1–3 plane is written as

$$-\frac{\sigma_{13}}{S_{13}} - 2\left(\frac{p}{S_{13}}\right)\sigma_{33} = 1 \tag{2}$$

where p is the experimental slope of the $(\sigma_{33}, \sigma_{13})$ fracture envelope for $\sigma_{33} \leq 0$.

Some research works have shown that composite materials that fail by transverse compressive failure follow the Mohr–Coulomb yield criterion reasonably well [19]. The Mohr–Coulomb criterion assumes that the shear failure stress on the fracture surface is equal to the bond strength plus the internal friction resistance, which is the result of the interaction of the internal friction coefficient and normal stress. Some literature demonstrated the validity of this criterion through the failure of composites under lateral compression.

$$\tau_{13} = S_{13} - \eta\sigma_{33} \tag{3}$$

$$\eta = -\frac{1}{\tan 2\alpha_0} \tag{4}$$

where η is the influence factor of normal stress acting perpendicular to the fracture surface. α_o is the fracture surface angle. Puck and Schürmann determined that most unidirectional graphite/epoxy composites fail by transverse shear along a fracture plane oriented at $\alpha_o = 53 \pm 2^\circ$. The parameter η that controls this angle can also be obtained through additional testing. However, Puck and Schürmann differentiated the coefficients of influence η_T and η_L for transverse shear S_T and longitudinal shear S_L, respectively. η_T can be determined from a uniaxial transverse compression experiment using Eq. (4), while η_L can be determined from shear experiments with varying degrees of transverse compression [20]. In the absence of the biaxial experiment data, η_L can be estimated from the longitudinal and transverse shear strengths and the transverse compressive strength Y_c [21].

$$\frac{\eta_L}{S_L} = \frac{\eta_T}{S_T} \Rightarrow \eta_L = -\frac{S_L \cos 2\alpha_o}{Y_c \cos^2 \alpha_o} \tag{5}$$

In addition to this failure criterion, Christensen and DeTeresa developed an out-of-plane delamination criterion accounting for the strengthening effect of through-thickness compression on interlaminar shear strength [19].

$$-\frac{\sigma_{33}}{T} + \frac{\sigma_{13}^2 + \sigma_{23}^2}{S^2} = 1 \tag{6}$$

Where T is the transverse tensile strength and S is the pure interlaminar shear strength. T is estimated as the in-plane transverse tensile strength of a unidirectional lamina. S is measured in the experiment for a particular laminate and no distinction was made if it is the longitudinal or the transverse interlaminar shear strength. σ are the stresses with the conventional index notation for the composites.

Daniel *et al.* argued that delamination damage was primarily influenced by the resin strength. Accordingly, a criterion based on transverse tensile stress was proposed (Northwestern University (NU) theory) [22]. This criterion was validated by the interlaminar shear strength enhancement experiment of the braid composite under normal stress. The results showed that this failure criterion agreed well with the experimental results. The expression of this criterion is as follows:

$$\sigma_{13} = S_{13}\sqrt{1 - \frac{2G_{13}}{E_3 S_{13}}\sigma_{13}} \tag{7}$$

where S_{13} is the pure interlaminar shear strength. G_{13} and E_3 are the out-of-plane shear and elastic moduli, respectively. A similar variant of the failure criterion can also be derived based on the ultimate principal tensile stress or principal tensile strain energy.

Tsai–Wu tensor criterion also reflects the influence of interlaminar normal stress on interlaminar shear strength of composites [23], which is expressed as follows:

$$f(\sigma_i) = F_i\sigma_i + F_{ij}\sigma_i\sigma_j + F_{ijk}\sigma_i\sigma_j\sigma_k + \ldots = 1 \tag{8}$$

The double-notch shear specimen is mainly in the plane stress state. thus, there are mainly normal stress perpendicular to the fibre direction and interlaminar shear stress on the shear plane. The Tsai–Wu tensor criterion can be expressed as follows:

$$\left(\frac{1}{S_2^+} - \frac{1}{S_2^-}\right)\sigma_2 + \left(\frac{\sigma_2}{S_2^- S_2^+}\right)^2 + \left(\frac{\tau_{12}}{S_{12}}\right)^2 = 1 \tag{9}$$

where S_1^+ is the tensile strength in the direction of the fibre, S_1^- is the compressive strength in the direction of the fibre, S_2^+ is the tensile strength in the direction perpendicular to the fibre, S_2^+ is the compressive strength in the direction perpendicular to the fibre, and S_{12} is the shear strength.

Envelope diagrams with different failure criteria could be obtained, as shown in Figure 15. In this figure, the horizontal axis is normal stress. A positive value represents tensile normal stress and a negative value represents a compressive normal stress. It can be seen from the envelope diagram that the above-mentioned criteria could all describe the effect of normal stress on the interlaminar strength relatively well. When normal stress was a compressive stress, normal stress has an enhancing effect on interlaminar shear strength, *i.e.* as normal stress increases, the interlaminar shear strength of the material also increases. When normal stress was a tensile stress, normal stress has a weakening effect on interlaminar shear strength, *i.e.* as tensile normal stress increases, the interlaminar shear strength of the material decreases.

Figure 16 shows a comparison of the original experimental data with the failure criteria. It can be seen from the

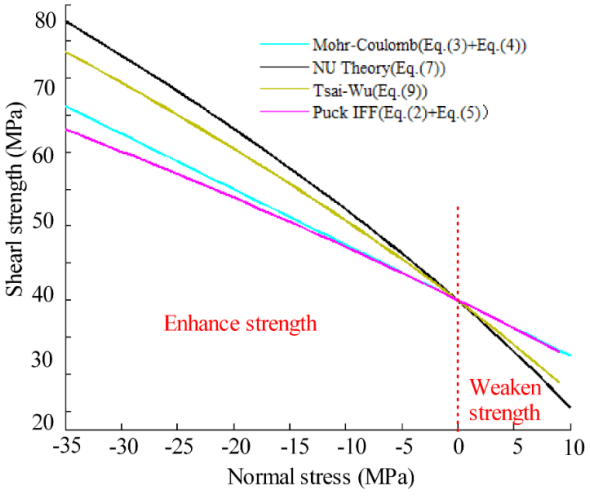

Figure 15: Relationship between normal stress and interlaminar shear strength under different failure criteria

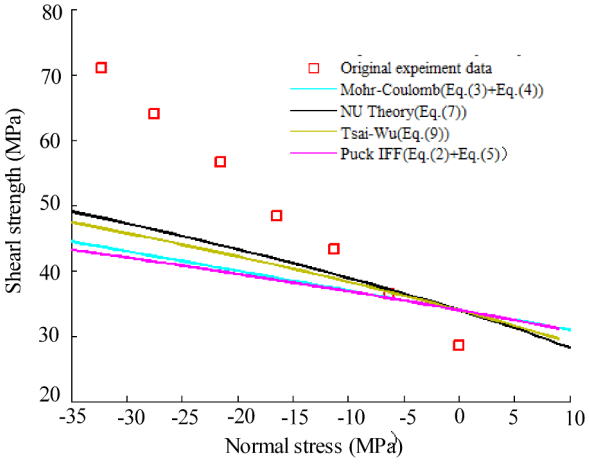

Figure 16: Comparison of original experimental data and failure criteria

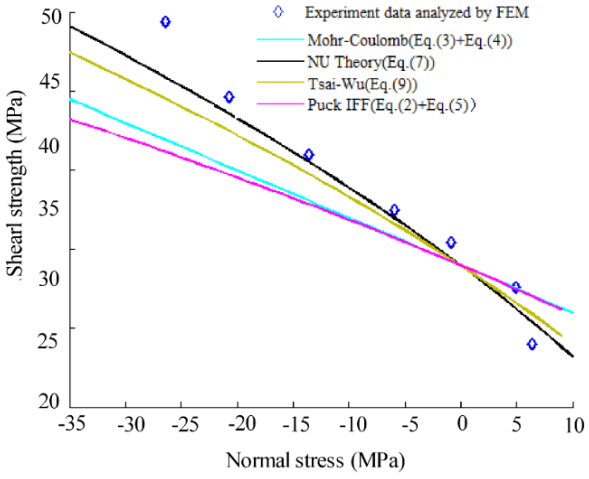

Figure 17: Comparison of failure criteria and experimental data analyzed by FEM

figure that the original experimental data is in good agreement with the existing failure criteria in term of change trend. This means that the compressive normal stress has an enhancing effect on interlaminar shear strength, and the tensile normal stress has a weakening effect on interlaminar shear strength. This proves that the double-notch shear specimen improved in this study can be used to study the influence mechanism of normal stress on the interlaminar shear strength of composites effectively. However, the original experimental data is numerically different from the failure criteria, with a maximum difference of 50%. The main reason is that the original data did not consider the influence of normal stress on the specimen shear plane and the friction between the interfaces of the external normal stress application device and the composite material. Therefore, the externally applied normal stress and average shear strength cannot be directly used in this type of experiment to study the influence mechanism of normal stress on interlaminar shear strength.

Figure 17 shows a comparison of the experimental data processed by the finite element method and that by the failure criteria. It can be seen from the figure that the processed data is in good agreement with the existing failure criteria both in term of change trend and numerical value. The variation patterns of the two both showed that the compressive normal stress enhanced interlaminar shear strength, and the tensile normal stress weakened interlaminar shear strength. Numerically, the experimental data obtained in this study agreed best with the NU theory criterion, with a maximum numerical difference of 4%. The obtained data differed most with the Puckand Schürmann criterion, with a maximum numerical difference of 13.6%. However, regardless of the criterion, the maximum numerical value was not more than 15%. This proves that the characteristic curve method proposed in this study could effectively eliminate the influence of normal stress and friction on interlaminar shear strength, thereby accurately reflecting the relationship between normal stress and interlaminar shear strength in the double-notch shear specimen. And the NU theory criterion can reflect the influence mechanism of the composite interlaminar shear strength best.

4 Conclusions

In this study, the Influence mechanism of composite interlaminar shear strength under the normal stress was studied through an improved double-notch shear experiment.

The characteristic curve method based on a double-notch shear specimen was proposed to study the influence of normal stress on the shear plane and friction on interlaminar shear strength. The resultant experimental data was compared with the existing failure criteria. Based on this study, the following conclusions are drawn:

1. The improved double-notch shear specimen can effectively study the influence mechanism of composite interlaminar shear strength under normal stress.
2. Based on the characteristic curve method, The experimental data analyzed by FEM agreed best with the NU theory criterion, with a maximum numerical difference of 4%, and differed most from the Puckand Schürmann criterion, with a maximum difference of 13.6%. And the NU theory criterion can reflect the influence mechanism of the composite interlaminar shear strength best.
3. The compressive normal stress has an enhancing effect on interlaminar shear strength, and the tensile normal stress has a weakening effect on interlaminar shear strength. Therefore, the generation of the tensile normal stress should be avoided as much as possible in the composite structure.

Acknowledgement: This work was financially supported by National Science Foundation of China under Grant (No.11702324), and Chongqing science and Technology Bureau of china (No. KJQN201900714).

References

[1] Votsis Renos A, Stratford Tim J, *et al.* Dynamic assessment of a FRP suspension footbridge through field testing and finite element modelling. Steel Compos Struct., vol. 187, no. 23, pp. 205-215,2018.

[2] Dongdong Zhang, *et al.* Torsional behaviour of a hybrid FRP-aluminum space truss bridge: Experimental and numerical study. Eng Struct., vol. 157, no. 13, pp. 132-143,2018;

[3] Mehdi Zomorodian, Guang Yang, Abdeldje lilBelarbi, Ashraf Ayoub. Behavior of FRP-strengthened RC elements subjected to pure shear. Constr Build Mater., vol. 170, no. 38, pp.378-391,2018.

[4] Bo Zhang, Yong Li, Nicholas Fantuzzi *et al.* Investigation of the Flow Properties of CBM Based on Stochastic Fracture Network Modeling. MATERIALS., vol.12, no.15, pp. 2387-2392,2019.

[5] Bibekananda Mandal, Anupam Chakrabarti. Numerical failure assessment of multi-bolt FRP composite joints with varying sizes and preloads of bolts. Compos Struct.; vol. 187, no.25, pp.169-178, 2017.

[6] Jiaxin Lv, Yi Xiao, Yuande Xue. Time–temperature-dependent response and analysis of preload relaxation in bolted composite joints. J Reinf Plast Comp., vol. 37, no. 25, pp. 460-474, 2018.

[7] Emre Çiplak, Onur Sayman. Failure Load of Mechanically Fastened Immersed Composite Laminated Plates under a Preloaded Moment. Polym Polym Compos., vol. 19, no. 5, pp. 41-46, 2018.

[8] Libin Zhaoa,b, Ziang Fanga. A modified stiffness method considering effects of hole tensile deformation on bolt load distribution in multi-bolt composite joints. Compos Struct., vol. 171, no.38, pp.264-271, 2019.

[9] F. Li *et al.* Experimental investigation of novel pre-tightened teeth connection technique for composite tube. Steel Compos Struct., vol. 23, no. 12, pp. 161-172, 2017.

[10] McManamy TJ, Kanemoto G, Snook P. Insulation irradiation test program for the compact ignition tokamak Cryogenics. Cryogenics., vol. 31, no. 13, pp. 277–281, 1991.

[11] DeTeresa SJ, Freeman DC, Groves SE. The effects of through-thickness compression on the interlaminar shear response of laminated fiber composites. J Compos Mater., vol. 38, no. 17, pp. 681–697, 2004.

[12] Hine PJ, Duckett RA, Kaddour AS, Hinton MJ, Wells GM. The effect of hydrostatic pressure on the mechanical properties of glass fiber/epoxy unidirectional composites. Compos Part A-Appl S., vol. 36, no. 7, pp. 279–289, 2005.

[13] Koerber H, Xavier J, Camanho PP. High strain rate characterization of unidirectional carbon-epoxy IM7-8552 in transverse compression and in plane shear using digital image correlation. Mech Mater., vol. 42, no. 11, pp. 1004–1019, 2010.

[14] Khong Wui Gan, Stephen R. Hallet *et al.* Measurement and modelling of interlaminar shear strength enhancement under moderate through-thickness compression. Compos Part A-Appl S., vol. 49, no. 12, pp. 18-25, 2013.

[15] Jin-Hwe Kweon, Hyon-Su Ahn, Jin-Ho choi. A new method to determine the characteristic length of composite joint without testing. Compos Struct ., vol. 56, no. 3, pp. 305-315, 2004.

[16] F. Li et al. A prediction method of the failure load and failure mode for composite pre-tightened tooth connections based on the characteristic lengths. Compos Struct., vol. 15, no. 21, pp. 684-693, 2016.

[17] Yifeng G, Fei L, Qilin Z, Jiangang G, and Yubo H. Strength Prediction of a Single Tooth Bound to Composite Pre-tightened Tooth Connection (PTTC) Joints based on Different Failure Criteria. Ksce J Civ Eng., vol. 23, no. 20, pp. 3547-3559,2019.

[18] Puck A, Schurmann H. Failure analysis of FRP laminates by means of physically based phenomenological models. Compos Sci Technol., vol. 62, no. 16, pp. 1633–1662, 2002.

[19] Bazhenov SL, Kozey VV. Transversal compression fracture of unidirectional fiber-reinforced plastics. J Mater Sci., vol. 26, no. 10, pp. 2677–2684, 1991.

[20] Davila CG, Camanho PP, Rose CA. Failure criteria for FRP laminates. J Compos Mater., vol. 39, no. 8, pp. 323–345, 2005.

[21] Christensen RM, DeTeresa SJ. Delamination failure investigation for out-of plane loading in laminates. J Compos Mater., vol. 38, no. 14, pp. 2231–2238, 2004.

[22] Daniel IM, Luo J-J, Schubel PM. Three-dimensional characterization of textile composites. Compos Part B-Eng ., vol. 39, no.21 pp. 13–19, 2008.

[23] Shen Guanlin, Mechanic of composite materials, Tsinghua University Press, 2013.